3
Two-Terminal Transmission System

3.1 INTRODUCTION

The performance of power system is affected by faults on transmission lines which results in disturbance of power flow. Hence there is need for quick detection and classification of fault, such that the performance and the reliability of power system can be improved by clearing of the fault. Two-terminal transmission systems are most prominently used for transmission of power from one node to another.

3.2 SYSTEM MODEL AND PARAMETERS

The single line diagram of the two-terminal system, considered, along with various blocks of the proposed scheme, is shown in Figure 3.1. The Transmission system under consideration has a voltage rating of 500kVAC and operates at a power frequency of 60Hz, connecting two AC systems. The parameters of the system are given in Table 3.1.

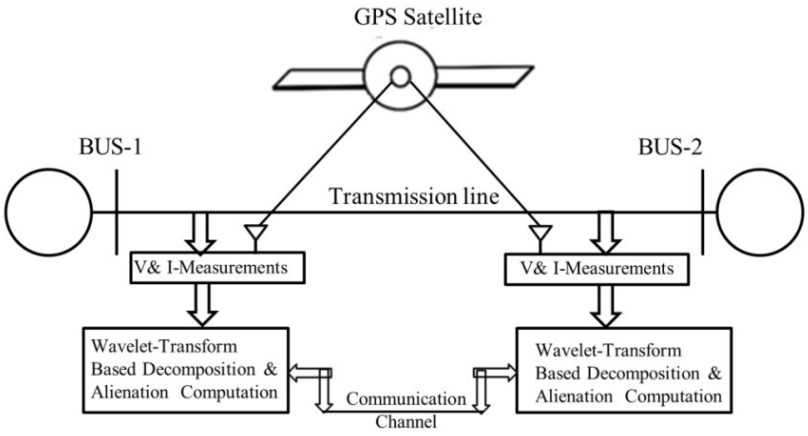

Figure 3.1 : System under consideration

Table 3.1: System Parameters

Transmission Line Length	230Km
Source at Bus-1	
Source Voltage	500 ∠20°kV
Source Impedance (Z_{s1})	17.177+j45.529Ω
Ac Source-2:	
Source Voltage	500∠0°kV
Source Impedance (Z_{s2})	15.31+j45.925Ω
Transmission Line Parameters	
Z_1	4.983+j117.83Ω
Z_0	12.682+j364.196Ω
Y_1	j1.468mʊ
Y_0	j1.099mʊ
Total Power	433.63(MW)+ j294.52 (MVAR)

3.3 WAVELET-ALIENATION BASED ALGORITHM

The three-phase currents of local and remote ends of transmission line are sampled at 1920Hz. The synchronization of sampling process is accomplished with the help of GPS clock. These current samples are obtained over a moving window of quarter cycle length. These current samples are decomposed with db2 mother wavelet to obtain approximate coefficients of first level (A_1). Alienation coefficient, A_α is computed by comparing the approximate coefficients of current window, W_0 (obtained at t_0), with those of the previous window, W_{-1} (obtained at $(-T+t_0)$) as shown in Figure 3.2, where, T represents the time period of the signal.

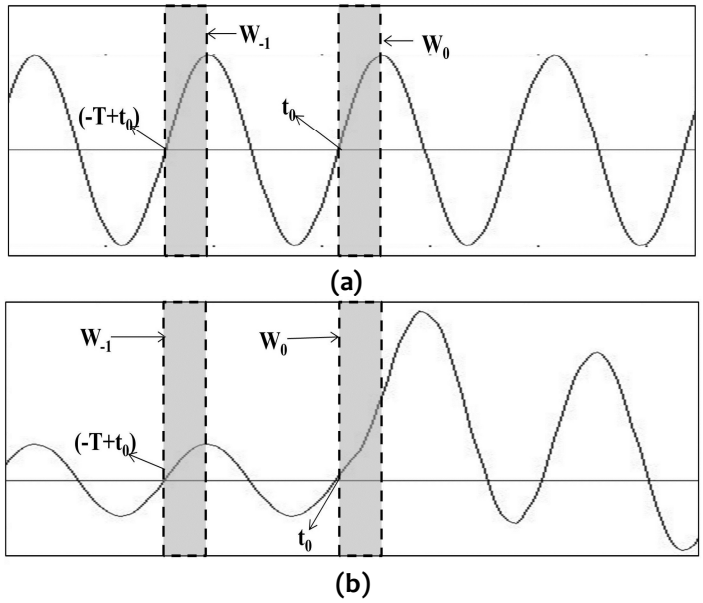

Figure 3.2*: Comparison windows for alienation coefficients: (*a) Without Fault, and (b) With Fault at t_o

Under normal conditions, the values of A_α remains zero since the two successive windows have same set of approximate coefficients. In the event of a fault, the approximate coefficients of current window would differ from those of preceding window. Thus, alienation coefficient would increase from zero to a finite value indicating fault. The fault Indexes of all the three phases are obtained by adding alienation coefficients of local and remote end currents. This fault index is compared with a threshold (F-TH=0.2) value to detect the faulty phase. Thus, the faulty phase would have fault index greater than the threshold whereas the fault index of healthy phase would be less than the threshold. The flow chart for the proposed algorithm is illustrated in Figure 3.3.

3.4 DETECTION AND CLASSIFICATION OF FAULTS

Simulation has been carried out for 10-cycles. Faults have been simulated after 5-cycles to obtain post fault transients for 5-cycles. Figure 3.4 demonstrates the performance of proposed algorithm in case of AG fault at the middle of transmission line. Figures 3.4 (a) and 3.4 (b) show the variation of three phase currents for AG fault at bus-1 and bus-2 respectively. Figures 3.3 (c) and 3.4 (d) illustrate the variation of approximation coefficients (A_1) with time for three-phase currents at bus-1 and bus-2 respectively. Figures 3.4 (e) and 3.4 (f) illustrate the variation of alienation coefficients with time at bus-1 and bus-2 respectively. Figure 3.4 (g) shows the fault index variation at each bus. It can be observed that the fault index of phase-A is greater than the threshold and those of phase-B and phase-C are below threshold (F-TH). Thus, the proposed scheme detects and classifies the fault as line to ground fault (AG Fault).

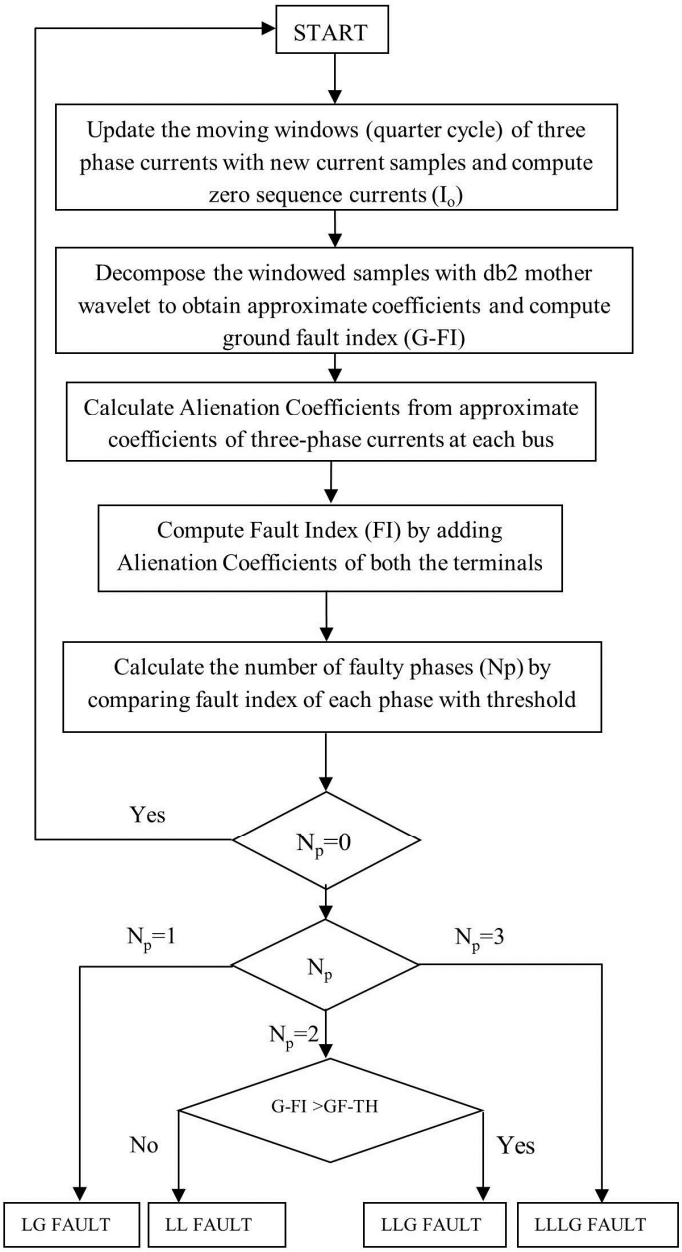

Figure 3.3: Flow chart of proposed scheme

Figure 3.5 illustrates the detection and classification of various types of faults on transmission line. Figures 3.5 (a) and 3.5 (b) show the fault index variation for BG and CG faults respectively, in which fault index of only faulty phase is greater than the threshold and not for the healthy phases. Figures 3.5(c) and 3.5(f) depict the variation of three-phase fault indexes for AB and ABG faults respectively. Form these figures, it is evident that phase-A and phase-B have fault index greater than the threshold. Similarly, Figures 3.5 (d) and 3.5 (g) illustrate the fault index variation for BC and BCG faults respectively, from which it can observed that fault indexes of faulty phases (phase-B & C) are greater than the threshold and not for healthy phase i.e. Phase-A. The fault index variation for AC and ACG faults is shown in Figures 3.5 (e) and 3.5 (h), from these figures it is depicted that fault index for phase-A and phase-C, are greater than the threshold whereas for phase-B it remains lower than the threshold, hence faults are identified as AC and ACG fault respectively. From Figure 3.6, it is evident that all the three phases have fault index values greater than the threshold, thus it is detected and classified as ABCG fault.

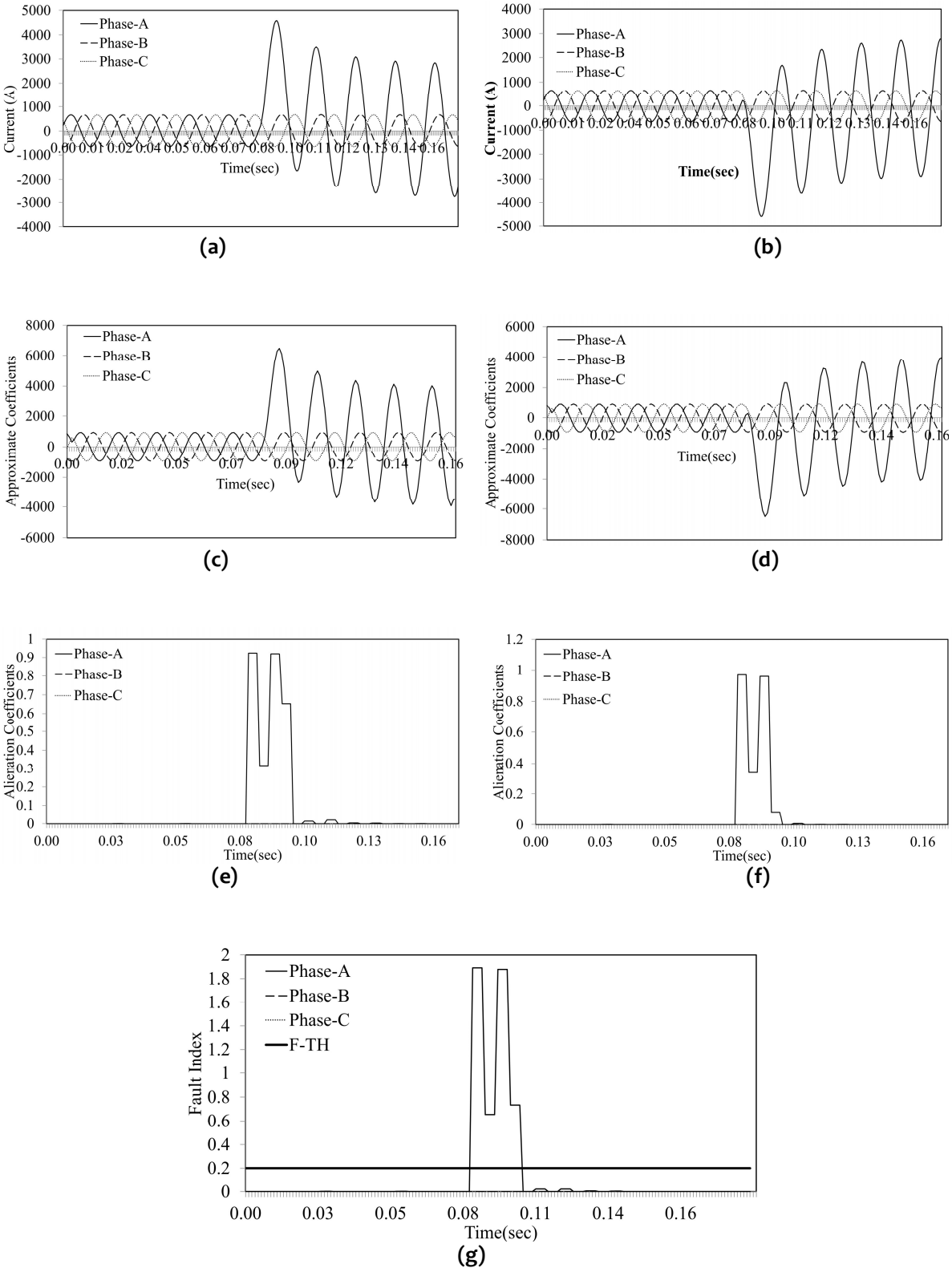

Figure 3.4: Detection of AG Fault: (a) Three-phase currents at Bus-1, (b) Three-phase currents at Bus-2, (c) Approximate Coefficients for Phase-A current at Bus-1, (d) Approximate Coefficients for Phase-A current at Bus-2, (e)Alienation Coefficients of approximate coefficients at Bus-1, (f) Alienation Coefficients of approximate coefficients at Bus-2, (g) Fault Index variation with time

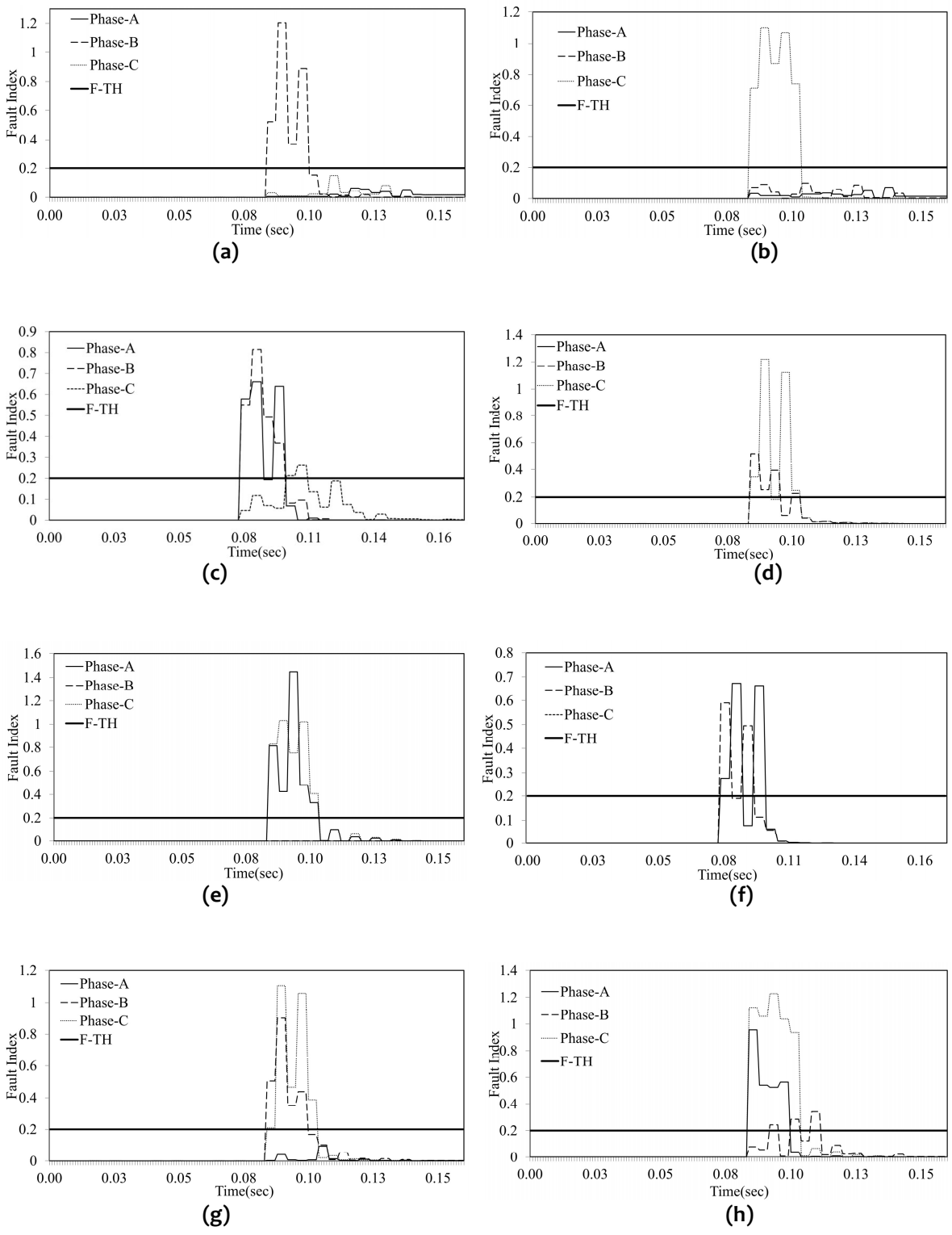

Figure 3.5: Variation of Fault Index with time: (a) BG Fault, (b) CG Fault, (c) AB Fault, (d) BC Fault, (e) AC Fault, (f) ABG Fault, (g) BCG Fault, (h) ACG Fault

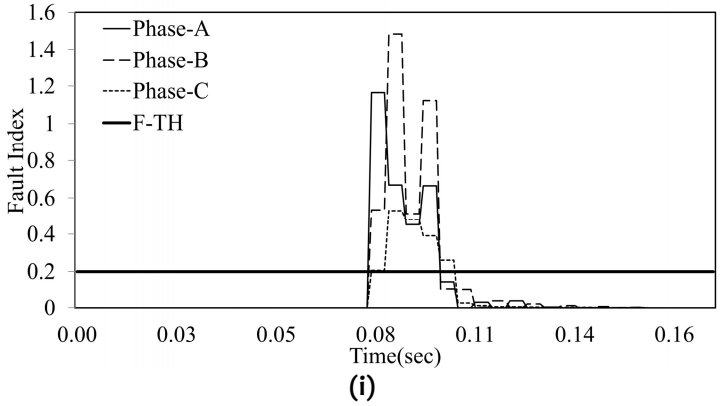

Figure 3.6: Variation of Fault Index with time for ABCG Fault

However, the discrimination between LL and LLG faults cannot be achieved by fault index alone. To discriminate between LL and LLG faults, zero sequence current is decomposed with same mother wavelet to obtain approximate coefficients (A_1) of first level and these are compared with ground fault threshold (GF-TH) to discriminate LLG from LL fault. From Figure 3.7, it is evident that the approximate coefficients in case of LLG fault exceed the GF-TH whereas for LL fault remains very low compared to GF-TH. Thus, LL faults can be discriminated from LLG faults with the help of zero sequence current.

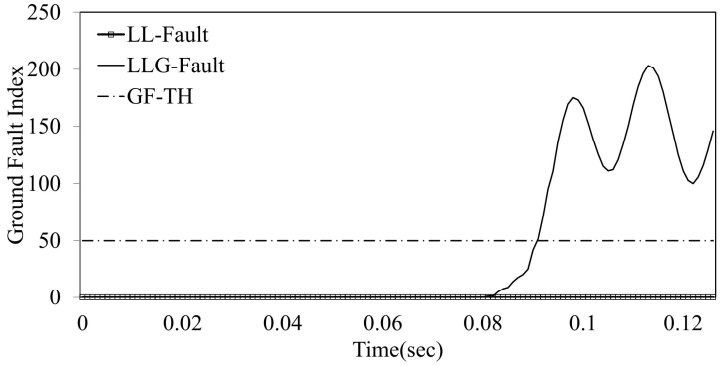

Figure 3.7: Discrimination between LL and LLG Fault

3.5 CASE STUDIES

All the ten types of faults i.e. LG, LL, LLG and LLLG have been simulated on transmission line. Variations in fault locations, fault incidence angles and fault impedance have been considered to establish the effectiveness of proposed scheme.

3.5.1 Variation of Fault Location

The post fault current transients are largely dependent on fault locations. Hence, there is a need to test the algorithm for faults at various locations of line. In this work, faults have been simulated at regular interval of 30km length of line. Figure 3.7 illustrates variation of fault indexes of three phases with fault location. From Figure 3.7 (a) it is evident that fault index of phase-A is always greater than the threshold for various locations of fault. Figures 3.7 (b) and 3.7 (c) show that the fault index of phase-A and phase-B are above the threshold value for various fault locations for AB and ABG faults respectively. From Figure 3.7 (d), it can be observed that for all the three phases, fault indexes are above the threshold value for various fault locations in case of ABCG fault.

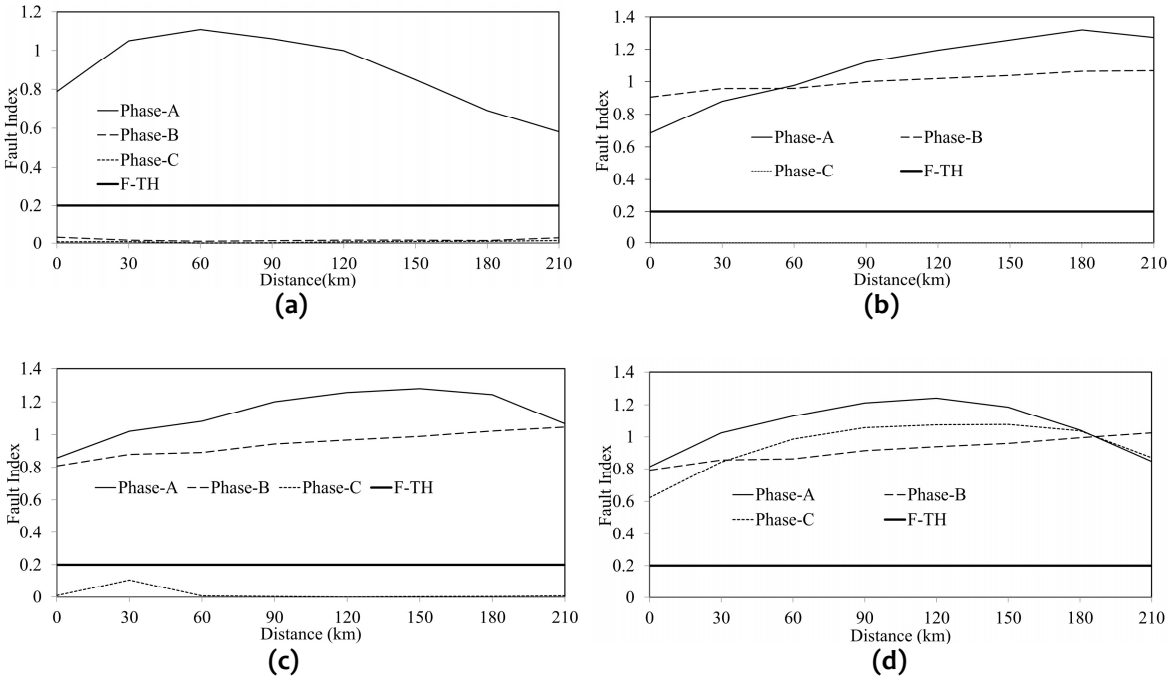

Figure 3.8: Variation of fault index with distance for three phase currents: (a) AG Fault, (b) AB Fault, (c) ABG Fault, (d) ABCG Fault

3.5.2 Variation of Fault Incidence Angle

The post fault current transients are dependent on fault incidence angle also. Hence, there is a need to test the algorithm for faults at various fault incidence angles. In this work, faults have been simulated at regular interval of 30° to test the proposed algorithm. Figure 3.9 illustrates variation of fault indexes of three phases with fault incidence angle.

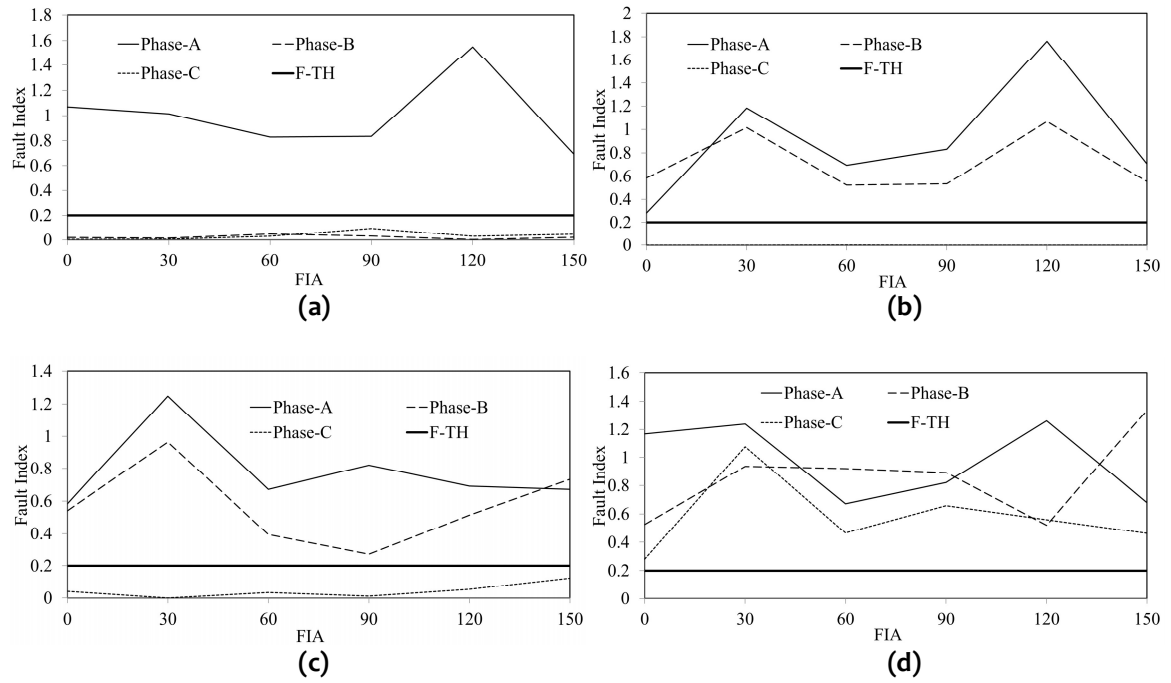

Figure 3.9: Variation of fault index for varying fault incidence angle (FIA): (a) AG Fault, (b) AB Fault, (c) ABG Fault, (d) ABCG Fault

From Figure 3.9 (a), it is evident that the fault index of phase-A is always greater than threshold for various fault incidence angles for AG fault. Figure 3.9 (b) and Figure 3.9 (c) illustrate that the fault index of phase-A and phase-B are above threshold value for various fault incidence angles for AB and ABG faults respectively. From Figure 3.9 (d) it can be observed that for all the three phases fault indexes are above threshold value for various fault incidence angles in case of ABCG fault.

Tables 3.2 to 3.11 demonstrate the successful performance of proposed algorithm for all the types of faults at different locations and with variations in incidence angle.

Table 3.2: Fault Index Variation with different locations and fault incidence angles for AG Fault

FIA	0			30			60			90			120			150		
Location	A	B	C	A	B	C	A	B	C	A	B	C	A	B	C	A	B	C
30	**1.05**	0.02	0.01	**0.75**	0.05	0.01	**0.69**	0.02	0.10	**0.86**	0.03	0.07	**0.63**	0.12	0.00	**0.88**	0.17	0.01
60	**1.11**	0.01	0.00	**0.91**	0.06	0.01	**0.62**	0.03	0.07	**0.93**	0.12	0.06	**0.57**	0.03	0.03	**0.81**	0.04	0.01
90	**1.06**	0.01	0.00	**1.17**	0.10	0.01	**0.65**	0.04	0.04	**0.70**	0.02	0.10	**0.56**	0.07	0.03	**0.72**	0.02	0.01
120	**1.00**	0.02	0.01	**1.33**	0.12	0.02	**0.75**	0.05	0.02	**0.54**	0.02	0.11	**0.43**	0.02	0.05	**0.64**	0.01	0.00
150	**0.85**	0.02	0.01	**1.31**	0.06	0.01	**0.67**	0.04	0.03	**0.68**	0.01	0.02	**0.51**	0.02	0.03	**0.57**	0.03	0.01
180	**0.69**	0.01	0.01	**1.23**	0.01	0.00	**0.68**	0.04	0.05	**0.78**	0.04	0.05	**0.47**	0.14	0.01	**0.52**	0.06	0.01
210	**0.58**	0.03	0.01	**1.03**	0.09	0.01	**0.74**	0.10	0.08	**0.86**	0.10	0.09	**0.44**	0.07	0.00	**0.49**	0.09	0.01

Table 3.3: Fault Index Variation with different locations and fault incidence angles for BG Fault

FIA	0			30			60			90			120			150		
Location	A	B	C	A	B	C	A	B	C	A	B	C	A	B	C	A	B	C
30	0.04	**0.64**	0.12	0.03	**1.25**	0.01	0.09	**0.92**	0.08	0.01	**0.95**	0.12	0.09	**0.88**	0.10	0.03	**0.54**	0.03
60	0.02	**0.51**	0.07	0.01	**1.46**	0.01	0.17	**0.86**	0.02	0.01	**0.98**	0.05	0.08	**0.83**	0.01	0.02	**0.49**	0.06
90	0.02	**0.49**	0.06	0.03	**1.56**	0.01	0.02	**0.92**	0.02	0.01	**1.06**	0.02	0.10	**1.05**	0.09	0.02	**0.46**	0.06
120	0.05	**0.54**	0.03	0.04	**1.66**	0.02	0.16	**1.06**	0.04	0.00	**1.15**	0.01	0.09	**1.12**	0.06	0.05	**0.51**	0.04
150	0.08	**0.59**	0.11	0.03	**1.84**	0.01	0.03	**1.02**	0.03	0.00	**0.59**	0.06	0.06	**1.18**	0.08	0.08	**0.57**	0.11
180	0.06	**0.55**	0.14	0.02	**1.96**	0.00	0.02	**1.08**	0.02	0.00	**1.05**	0.02	0.04	**1.18**	0.03	0.04	**1.21**	0.06
210	0.04	**0.48**	0.03	0.03	**1.73**	0.05	0.03	**1.20**	0.02	0.00	**0.71**	0.13	0.02	**0.89**	0.02	0.01	**1.18**	0.02

Table 3.4: Fault Index Variation with different locations and fault incidence angles for CG Fault

FIA	0			30			60			90			120			150		
Location	A	B	C	A	B	C	A	B	C	A	B	C	A	B	C	A	B	C
30	0.04	0.13	**1.18**	0.08	0.01	**1.10**	0.11	0.00	**1.06**	0.02	0.07	**1.54**	0.04	0.02	**0.56**	0.03	0.08	**0.30**
60	0.02	0.02	**1.06**	0.02	0.00	**1.09**	0.09	0.02	**1.08**	0.02	0.02	**1.51**	0.06	0.02	**0.51**	0.06	0.13	**0.48**
90	0.08	0.02	**0.92**	0.01	0.00	**1.08**	0.08	0.02	**1.09**	0.04	0.01	**1.45**	0.06	0.14	**0.62**	0.07	0.11	**0.47**
120	0.10	0.04	**0.84**	0.02	0.01	**1.09**	0.02	0.02	**1.07**	0.12	0.01	**1.35**	0.09	0.10	**0.47**	0.04	0.09	**0.74**
150	0.10	0.13	**0.93**	0.04	0.00	**1.08**	0.02	0.01	**1.07**	0.13	0.01	**1.23**	0.09	0.13	**0.85**	0.08	0.09	**1.03**
180	0.02	0.10	**1.02**	0.08	0.00	**1.07**	0.08	0.00	**1.07**	0.04	0.03	**1.15**	0.09	0.04	**0.49**	0.08	0.09	**1.06**
210	0.06	0.09	**1.05**	0.10	0.00	**1.06**	0.10	0.00	**1.08**	0.02	0.05	**1.10**	0.00	0.00	**0.47**	0.04	0.07	**0.99**

Table 3.5: Fault Index Variation with different locations and fault incidence angles for AB Fault

FIA	0			30			60			90			120			150		
Location	A	B	C	A	B	C	A	B	C	A	B	C	A	B	C	A	B	C
30	**0.88**	**0.96**	0.00	**1.69**	**0.96**	0.00	**1.81**	**1.16**	0.00	**1.61**	**1.07**	0.00	**1.72**	**1.11**	0.00	**1.69**	**1.03**	0.00
60	**0.98**	**0.96**	0.00	**1.50**	**0.59**	0.00	**1.65**	**0.79**	0.00	**1.80**	**1.05**	0.00	**1.78**	**1.09**	0.00	**1.76**	**0.96**	0.00
90	**1.12**	**1.00**	0.00	**1.37**	**0.46**	0.00	**1.61**	**0.72**	0.00	**1.75**	**0.88**	0.00	**1.79**	**0.98**	0.00	**1.63**	**0.76**	0.00
120	**1.19**	**1.02**	0.00	**1.31**	**0.35**	0.00	**1.47**	**0.49**	0.00	**1.65**	**0.71**	0.00	**1.76**	**0.85**	0.00	**1.74**	**0.79**	0.00
150	**1.26**	**1.04**	0.00	**1.43**	**0.49**	0.00	**1.48**	**0.47**	0.00	**1.61**	**0.58**	0.00	**1.73**	**0.76**	0.00	**1.72**	**0.79**	0.00
180	**1.32**	**1.06**	0.00	**1.33**	**0.35**	0.00	**1.40**	**0.46**	0.00	**1.68**	**0.65**	0.00	**1.71**	**0.69**	0.00	**1.61**	**0.54**	0.00
210	**1.27**	**1.07**	0.00	**1.11**	**0.17**	0.00	**1.64**	**0.70**	0.00	**1.63**	**0.65**	0.00	**1.75**	**0.71**	0.00	**1.56**	**0.58**	0.00

Table 3.6: Fault Index Variation with different locations and fault incidence angles for BC Fault

FIA	0			30			60			90			120			150		
Location	A	B	C	A	B	C	A	B	C	A	B	C	A	B	C	A	B	C
30	0.00	**0.60**	**0.30**	0.00	**1.23**	**1.05**	0.00	**0.31**	**1.36**	0.00	**0.99**	**1.60**	0.00	**0.54**	**0.75**	0.00	**0.57**	**0.94**
60	0.00	**0.52**	**0.44**	0.00	**1.61**	**0.90**	0.00	**0.30**	**1.33**	0.00	**0.88**	**1.57**	0.00	**0.42**	**0.22**	0.00	**0.50**	**0.72**
90	0.00	**0.48**	**0.54**	0.00	**1.73**	**0.90**	0.00	**0.30**	**1.31**	0.00	**0.78**	**1.52**	0.00	**0.37**	**0.47**	0.00	**0.45**	**0.71**
120	0.00	**0.54**	**0.46**	0.00	**1.85**	**0.79**	0.00	**0.30**	**1.29**	0.00	**0.70**	**1.44**	0.00	**0.41**	**0.41**	0.00	**0.51**	**0.29**
150	0.00	**0.61**	**0.28**	0.00	**1.99**	**0.57**	0.00	**0.28**	**1.26**	0.00	**0.60**	**1.34**	0.00	**0.40**	**0.45**	0.00	**0.59**	**0.25**
180	0.00	**0.57**	**0.32**	0.00	**1.86**	**0.36**	0.00	**0.28**	**1.24**	0.00	**0.53**	**1.27**	0.00	**0.33**	**0.41**	0.00	**0.54**	**0.29**
210	0.00	**0.49**	**0.29**	0.00	**1.49**	**0.27**	0.00	**0.27**	**1.16**	0.00	**0.46**	**1.22**	0.00	**0.37**	**0.21**	0.00	**0.46**	**0.27**

Table 3.7: Fault Index Variation with different locations and fault incidence angles for AC Fault

FIA	0			30			60			90			120			150		
Location	A	B	C	A	B	C	A	B	C	A	B	C	A	B	C	A	B	C
30	**1.32**	0.00	**0.71**	**1.23**	0.00	**0.88**	**1.38**	0.00	**0.90**	**1.25**	0.00	**1.19**	**1.20**	0.00	**1.08**	**1.02**	0.00	**0.99**
60	**1.32**	0.00	**0.87**	**1.36**	0.00	**0.69**	**1.30**	0.00	**1.02**	**1.13**	0.00	**1.08**	**1.19**	0.00	**1.11**	**0.92**	0.00	**0.91**
90	**1.40**	0.00	**0.69**	**1.38**	0.00	**0.81**	**1.41**	0.00	**1.08**	**1.42**	0.00	**1.24**	**1.44**	0.00	**1.28**	**0.93**	0.00	**0.97**
120	**1.43**	0.00	**0.73**	**1.40**	0.00	**0.62**	**1.44**	0.00	**0.79**	**1.25**	0.00	**1.21**	**1.13**	0.00	**0.99**	**0.84**	0.00	**0.81**
150	**1.38**	0.00	**0.59**	**1.34**	0.00	**0.57**	**1.61**	0.00	**0.84**	**1.63**	0.00	**1.34**	**1.43**	0.00	**1.26**	**1.03**	0.00	**0.98**
180	**1.30**	0.00	**0.51**	**1.21**	0.00	**0.46**	**1.51**	0.00	**0.75**	**1.87**	0.00	**1.46**	**1.53**	0.00	**1.23**	**1.12**	0.00	**1.04**
210	**0.98**	0.00	**0.33**	**1.11**	0.00	**0.38**	**1.15**	0.00	**0.47**	**1.91**	0.00	**1.20**	**1.70**	0.00	**1.49**	**1.20**	0.00	**1.07**

Table 3.8: Fault Index Variation with different locations and fault incidence angles for ABG Fault

FIA	0			30			60			90			120			150		
Location	A	B	C	A	B	C	A	B	C	A	B	C	A	B	C	A	B	C
30	**1.02**	**0.88**	0.11	**0.70**	**0.95**	0.05	**0.79**	**1.11**	0.06	**0.24**	**0.50**	0.03	**0.28**	**0.41**	0.00	**0.54**	**0.55**	0.02
60	**1.08**	**0.89**	0.01	**0.82**	**1.19**	0.04	**0.73**	**1.21**	0.10	**0.29**	**0.75**	0.09	**0.28**	**0.39**	0.04	**0.50**	**0.49**	0.03
90	**1.20**	**0.94**	0.00	**0.70**	**1.11**	0.17	**0.74**	**1.17**	0.11	**0.39**	**0.27**	0.10	**0.27**	**0.36**	0.06	**0.48**	**0.47**	0.02
120	**1.26**	**0.97**	0.00	**0.90**	**1.41**	0.11	**0.85**	**1.27**	0.04	**0.54**	**0.46**	0.11	**0.25**	**0.38**	0.16	**0.46**	**0.51**	0.02
150	**1.28**	**0.99**	0.00	**0.73**	**1.25**	0.01	**0.74**	**1.02**	0.07	**0.67**	**0.58**	0.02	**0.29**	**0.36**	0.09	**0.42**	**0.53**	0.04
180	**1.24**	**1.02**	0.00	**0.94**	**1.32**	0.03	**0.78**	**1.16**	0.03	**0.77**	**0.20**	0.05	**0.29**	**0.34**	0.07	**0.41**	**0.49**	0.03
210	**1.07**	**1.05**	0.01	**0.75**	**1.55**	0.08	**0.87**	**1.42**	0.08	**0.85**	**0.60**	0.09	**0.32**	**0.33**	0.06	**0.44**	**0.44**	0.02

Table 3.9: Fault Index Variation with different locations and fault incidence angles for BCG Fault

FIA	0			30			60			90			120			150		
Location	A	B	C	A	B	C	A	B	C	A	B	C	A	B	C	A	B	C
30	0.07	**0.55**	**0.24**	0.01	**1.26**	**0.24**	0.17	**1.33**	**1.11**	0.01	**1.20**	**1.49**	0.07	**0.43**	**0.48**	0.06	**0.53**	**0.22**
60	0.02	**0.50**	**0.22**	0.01	**1.45**	**0.27**	0.00	**1.27**	**1.12**	0.02	**1.15**	**1.46**	0.05	**0.38**	**0.31**	0.02	**0.47**	**0.95**
90	0.01	**0.47**	**0.30**	0.02	**1.53**	**0.28**	0.13	**1.29**	**1.12**	0.05	**1.10**	**1.41**	0.03	**0.33**	**0.33**	0.01	**0.44**	**0.63**
120	0.00	**0.52**	**0.23**	0.02	**1.60**	**0.29**	0.09	**1.30**	**1.10**	0.14	**1.07**	**1.31**	0.04	**0.38**	**0.24**	0.00	**0.49**	**0.72**
150	0.00	**0.57**	**0.46**	0.02	**1.76**	**0.22**	0.07	**1.28**	**1.08**	0.12	**0.99**	**1.20**	0.02	**0.37**	**0.35**	0.00	**0.55**	**0.43**
180	0.01	**0.53**	**0.52**	0.01	**1.93**	**0.48**	0.09	**1.27**	**1.08**	0.04	**0.91**	**1.14**	0.01	**0.34**	**0.28**	0.01	**0.51**	**0.49**
210	0.02	**0.48**	**0.46**	0.01	**1.85**	**0.41**	0.09	**1.21**	**1.05**	0.08	**0.88**	**1.10**	0.02	**0.37**	**0.43**	0.02	**0.46**	**0.44**

Table 3.10: Fault Index Variation with different locations and fault incidence angles for ACG Fault

FIA	0			30			60			90			120			150		
Location	A	B	C	A	B	C	A	B	C	A	B	C	A	B	C	A	B	C
30	**1.18**	0.03	**0.79**	**0.75**	0.05	**0.67**	**0.63**	0.01	**1.01**	**0.23**	0.00	**1.45**	**1.25**	0.06	**1.04**	**1.18**	0.02	**0.73**
60	**1.12**	0.15	**1.27**	**0.90**	0.06	**0.31**	**0.56**	0.01	**1.04**	**0.23**	0.00	**1.42**	**1.14**	0.11	**1.04**	**1.13**	0.15	**1.25**
90	**1.05**	0.11	**1.26**	**1.15**	0.09	**0.84**	**0.55**	0.01	**1.06**	**0.27**	0.00	**1.37**	**1.08**	0.04	**1.32**	**1.06**	0.12	**1.25**
120	**0.94**	0.09	**1.10**	**1.31**	0.10	**0.40**	**0.62**	0.00	**1.03**	**0.37**	0.00	**1.26**	**0.98**	0.07	**1.13**	**0.95**	0.10	**1.11**
150	**0.85**	0.02	**1.03**	**1.30**	0.04	**0.81**	**0.57**	0.01	**1.04**	**0.49**	0.00	**1.16**	**1.02**	0.01	**1.30**	**0.86**	0.02	**1.05**
180	**0.76**	0.03	**1.03**	**1.21**	0.01	**0.69**	**0.59**	0.01	**1.05**	**0.58**	0.00	**1.10**	**0.89**	0.01	**1.08**	**0.77**	0.03	**1.05**
210	**0.62**	0.11	**1.07**	**1.02**	0.13	**0.26**	**0.66**	0.03	**1.07**	**0.67**	0.00	**1.05**	**0.76**	0.13	**1.10**	**0.64**	0.14	**1.09**

Table 3.11: Fault Index Variation with different locations and fault incidence angles for ABCG Fault

FIA	0			30			60			90			120			150		
Location	A	B	C	A	B	C	A	B	C	A	B	C	A	B	C	A	B	C
30	**1.03**	**0.86**	**0.84**	**0.61**	**1.27**	**1.07**	**0.71**	**1.14**	**1.04**	**0.23**	**0.68**	**1.43**	**0.52**	**0.41**	**0.73**	**0.68**	**0.53**	**0.37**
60	**1.13**	**0.86**	**0.99**	**0.68**	**1.36**	**1.06**	**0.64**	**1.12**	**1.06**	**0.24**	**0.75**	**1.41**	**0.49**	**0.37**	**0.56**	**0.64**	**0.47**	**0.38**
90	**1.21**	**0.91**	**1.06**	**0.60**	**1.05**	**1.06**	**0.63**	**1.21**	**1.08**	**0.27**	**0.84**	**1.35**	**0.51**	**0.33**	**0.66**	**0.61**	**0.44**	**0.29**
120	**1.24**	**0.94**	**1.08**	**0.72**	**1.43**	**1.07**	**0.72**	**1.40**	**1.05**	**0.38**	**0.91**	**1.25**	**0.43**	**0.37**	**0.48**	**0.57**	**0.49**	**0.38**
150	**1.19**	**0.96**	**1.08**	**0.62**	**1.17**	**1.06**	**0.64**	**1.38**	**1.05**	**0.50**	**0.94**	**1.15**	**0.52**	**0.35**	**0.69**	**0.54**	**0.52**	**0.73**
180	**1.04**	**0.99**	**1.04**	**0.72**	**1.35**	**1.06**	**0.67**	**1.43**	**1.06**	**0.59**	**1.00**	**1.09**	**0.49**	**0.33**	**0.48**	**0.53**	**0.49**	**0.78**
210	**0.85**	**1.03**	**0.87**	**0.64**	**1.34**	**1.06**	**0.74**	**1.50**	**1.07**	**0.68**	**1.03**	**1.05**	**0.48**	**0.35**	**0.64**	**0.52**	**0.44**	**0.67**

3.5.3 Variation of Fault Impedance

High impedance faults (HIF) are, in general, difficult to detect because of insensitivity of protection scheme to very low fault currents and/or limitations on other settings imposed. The proposed algorithm has been tested with fault impedances from 0-100 Ω. Figures 3.10-3.11 show the variation of fault index with time for three phases with fault impedance of 15Ω. Figure 3.10 (a) depicts that for phase-A (faulty phase) fault index is greater than the threshold and not for phase-B and phase-C (healthy phase), hence detects the fault as phase to ground (AG) fault. Figures 3.10 (b) and 3.10 (c) show the fault index variation for BG and CG faults respectively, in which fault index of faulty phase is greater than the threshold and not for the healthy phases. Figures 3.10 (d) and 3.11(a) depict the variation of three-phase fault indexes for AB and ABG faults respectively. Form these figures, it is evident that phase-A and phase-B have fault index greater than the threshold. Similarly, Figures 3.10 (e) and 3.11 (b) illustrate the fault index

variation for BC and BCG faults respectively, from which it can observed that fault indexes of faulty phases (phase-B & C) are greater than the threshold and not for healthy phase i.e. Phase-A. The fault index variation for AC and ACG faults, is shown in Figures 3.10 (f) and 3.11 (c), from these figures it is depicted that fault index for phase-A and phase-C are greater than the threshold whereas for phase-B it remains lower than the threshold, hence fault are identified as AC and ACG fault respectively. Figure 3.11 (d) shows that for all the three phases, fault index is greater than the threshold, hence it is detected as three phase to ground (ABCG) fault. Thus, it is evident that the fault impedance has no effect on proposed algorithm.

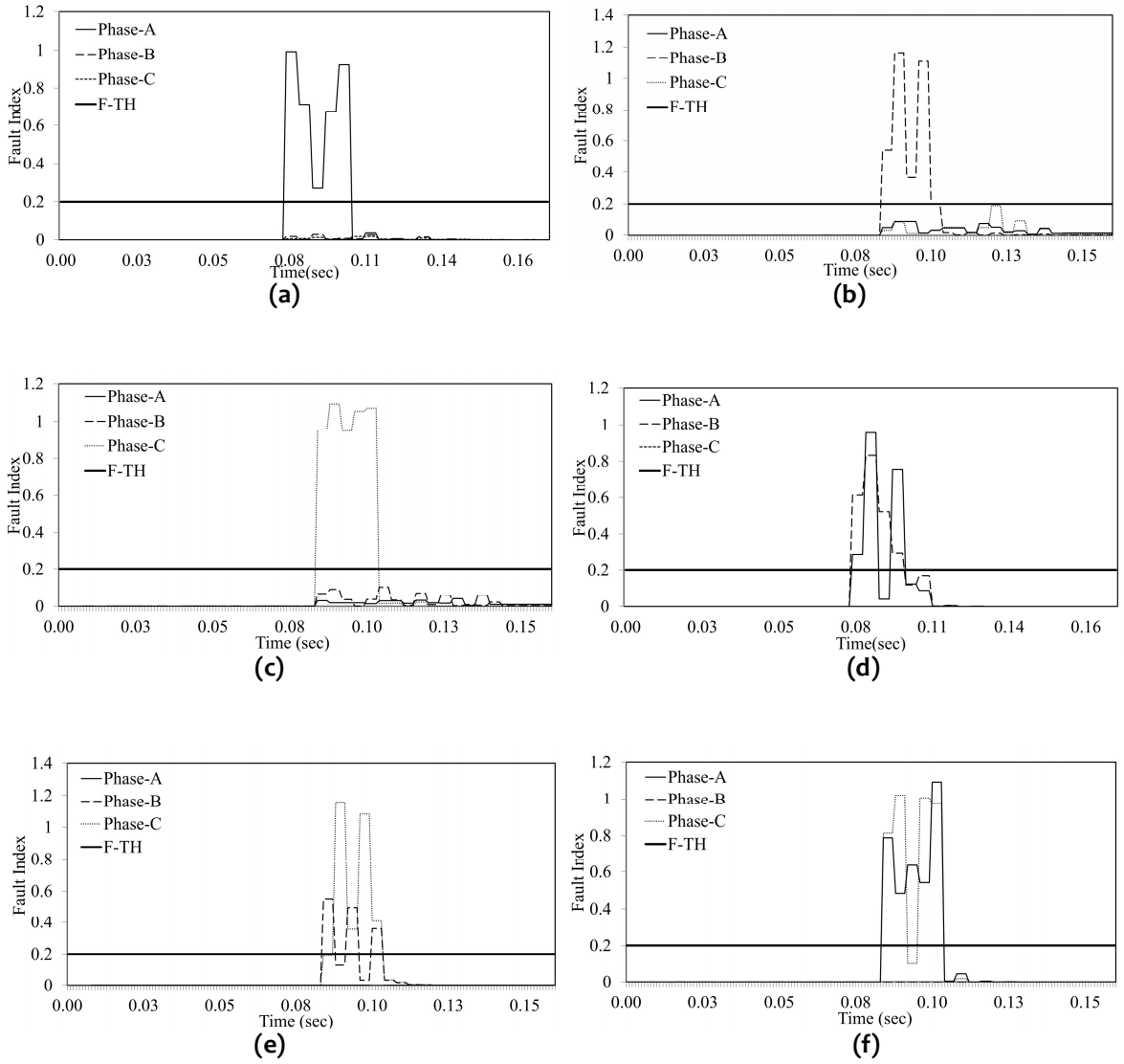

Figure 3.10: Variation of fault index with time for fault impedance of 15Ω: (a) AG Fault, (b) BG Fault, (c) CG Fault, (d) AB Fault, (e) BC Fault, (f) AC Fault

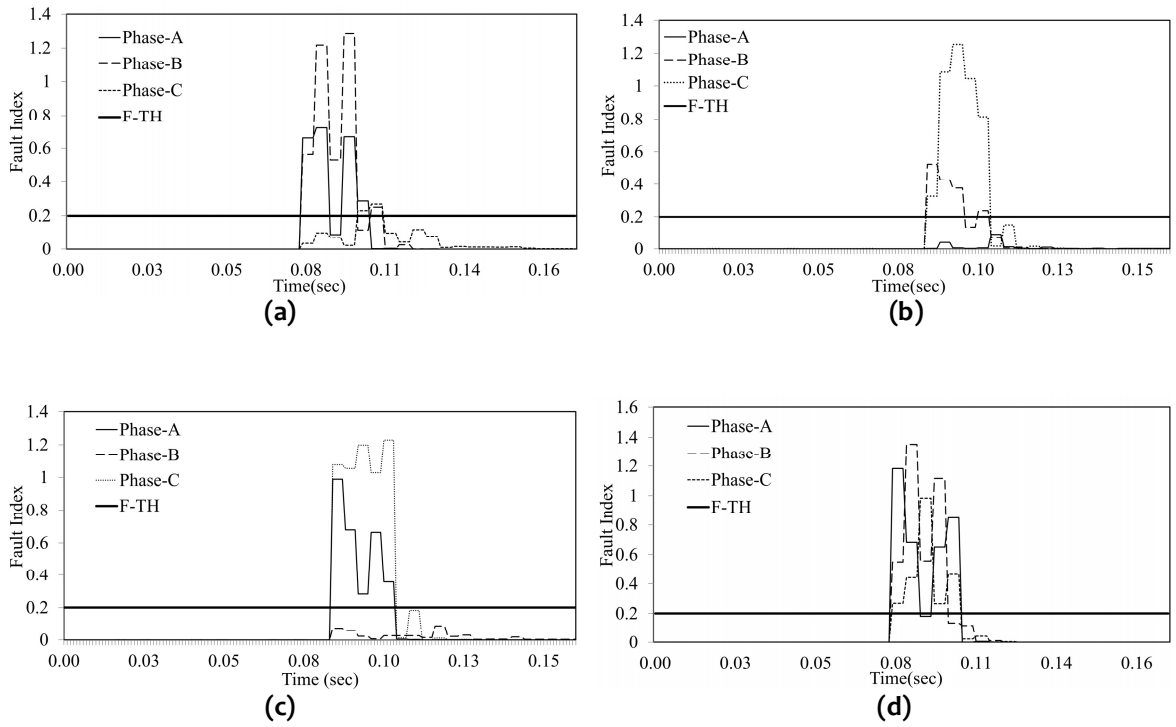

Figure 3.11: Variation of fault index with time for fault impedance of 15Ω: (a) ABG Fault, (b) BCG Fault, (c) ACG Fault, (d) ABCG Fault

3.5.4 Effect of Noise Contamination

The noise contamination effect on current signals has been examined for proposed algorithm, with different levels of noise. Figure 3.12 depicts variation of three-phase fault index for different types of faults, with 10dB and 20dB white Gaussian noise. Figure 3.12(a) depicts variation of fault index for AG fault. The fault index of phase-A is greater than the threshold and that of other phases is less than the threshold, thus illustrating AG fault. Figures 3.12(b) and 3.12 (c) illustrate that for phase-A and phase-B, fault index is greater than the threshold and not for phase-C, and hence the faults are detected as AB and ABG fault, respectively. Figure 3.12 (d) shows that for all the three phases, fault index is greater than the threshold. Hence it is detected as ABCG fault. Thus, it is evident that presence of noise in the current signals has no effect on proposed algorithm.

3.5.5 Effect of Loading

The proposed algorithm has been tested with load switching. It has been observed that for 10% and 20% load switching, the maximum values of fault index for phase-A, phase-B and phase-C are well below the threshold value. Fig 3.13 (a) and 3.13 (b) shows the effect of 10 % and 20 % loading for the proposed algorithm.

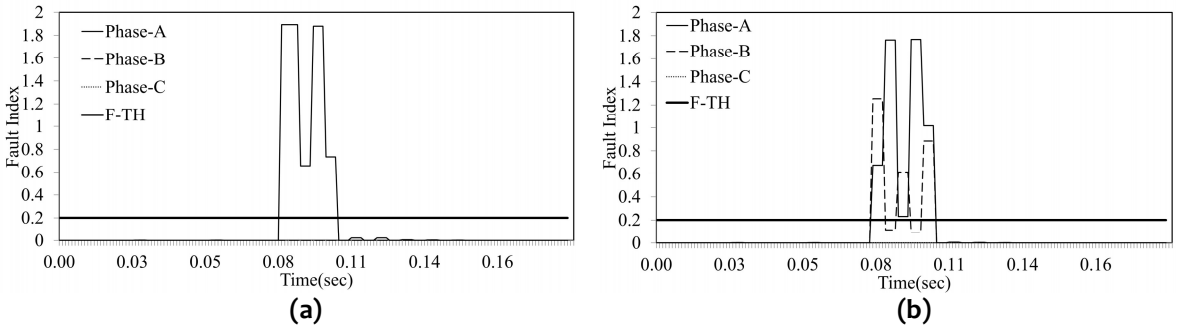

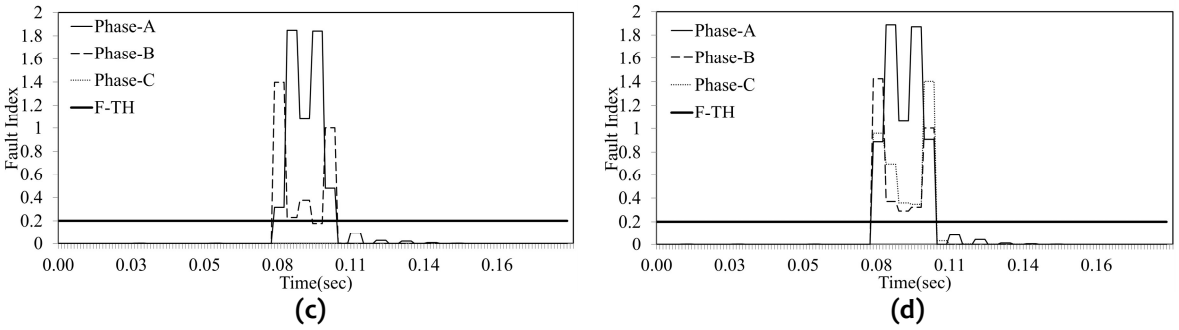

Figure 3.12: Variation of fault index with time for effect of noise: (a) ABG Fault, (b) BCG Fault, (c) ACG Fault, (d) ABCG Fault

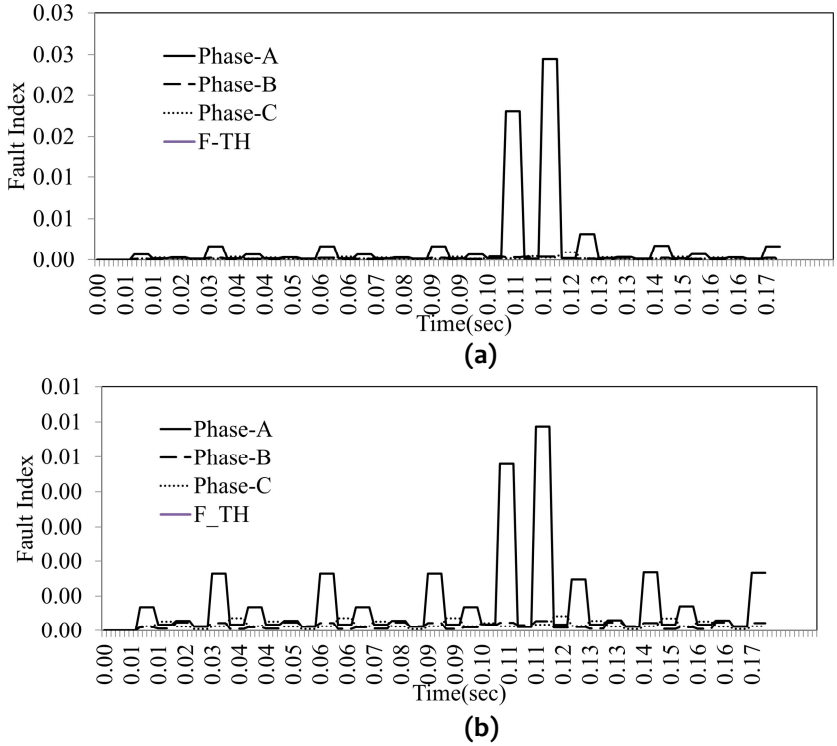

Figure 3.13: Variation of fault index with time for effect of loading

3.6 ESTIMATION OF FAULT LOCATION

Subsequent to detection and classification of a fault, estimation of fault location is carried out using Artificial Neural Network (ANN). For this purpose, the samples of voltage signals, obtained over a moving window of quarter cycle, are decomposed with db2 mother wavelet along with current signals. The approximate coefficients of voltage and current signals, obtained from these windows, followed by fault incidence, are fed as inputs to ANN. ANN is trained to yield fault location in kms, as output. A multi-layer perceptron model with Levenberg-Marquardt optimization method has been adopted for this purpose.

Two ANNs have been proposed to locate the fault, one making use of local bus data and the other making use of local and remote bus data. The proposed ANNs have one hidden layer as shown in Figure 3.14. The details related to number of neurons in input, hidden and output layers and their transfer functions are presented in Tables 3.12 and 3.13 for the two ANNs proposed.

The training of proposed ANN is carried out by feeding the data obtained from simulation of various faults at various locations and with different fault impedances. The testing

of ANN is carried out by simulating the faults at new locations. The % error in estimation of the fault location is computed as difference of ANN distance and actual distance expressed as percentage of total length of the line (L).

$$\%Error = \frac{|\ NNDis\tan ce - ActualDis\tan ce\ |}{L} * 100$$

The performance of ANN, which makes use of bus-1 data alone, without and with fault impedances, is presented in the Tables 3.14 and 3.15 respectively. Tables 3.16 and 3.17 illustrate the performance of ANN which makes use of bus-2 data alone, without and with fault impedances, respectively. From these Tables, it can be observed that the maximum and average errors are as low as 2.85% and 0.32% respectively.

The performance of ANN, which makes use of local and remote bus data, without and with fault impedances, is illustrated in Tables 3.18 and 3.19. From these tables, it is evident that the maximum and average errors can be reduced to as low as 1.51% and 0.24% respectively. From these comparative studies, it can be established that the ANN which makes use of local and remote bus data estimates the fault location with a greater accuracy. Table 3.20 presents the summary of the performance of various ANNs proposed.

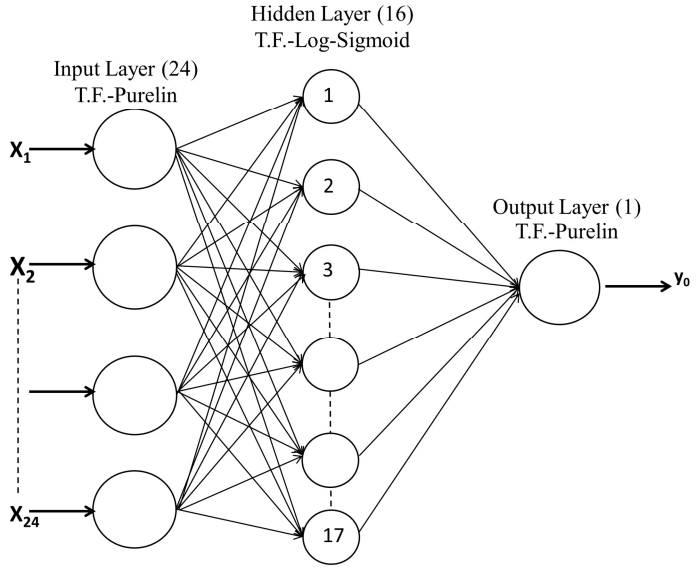

Figure 3.14: ANN Architecture

Table 3.12: Details of ANN making use of local bus data

Layer	Number of Neurons	Transfer Function
Input	24	Purelin
Hidden	16	Log-sigmoid
Output	1	Purelin

Table 3.13: Details of ANN making use of local and remote bus data

Layer	Number of Neurons	Transfer Function
Input	48	Purelin
Hidden	16	Log-sigmoid
Output	1	Purelin

Table 3.14: Performance of ANN using Bus-1 Data as Inputs for Solid Faults

S.No.	Actual Distance (in kms)	Phase-B to Ground Fault (BG)		Phase-B to Phase-C Fault (BC)		Phases-B and C to Ground Fault (BCG)		Three-Phase Fault (ABCG)	
		ANN Distance (in kms)	% Error	ANN Distance (in kms)	% Error	ANN Distance (in kms)	% Error	ANN Distance (in kms)	% Error
1.	55	54.70	0.130	50.24	2.069	52.39	1.134	55.64	0.278
2.	95	94.60	0.173	93.82	0.513	94.55	0.019	93.07	0.839
3.	135	135.01	0.004	134.91	0.039	134.79	0.091	134.91	0.039
4.	175	175.16	0.069	175.00	0.000	181.28	2.730	174.99	0.004
5.	215	214.94	0.026	215.08	0.034	214.96	0.017	215.02	0.008

Table 3.15: Performance of ANN using Bus-1 Data as Inputs for High Impedance Faults (Z_f=15 Ω)

S.No.	Actual Distance (in kms)	Phase-B to Ground Fault (BG)		Phase-B to Phase-C Fault (BC)		Phases-B and C to Ground Fault (BCG)		Three-Phase Fault (ABCG)	
		ANN Distance (in kms)	% Error	ANN Distance (in kms)	% Error	ANN Distance (in kms)	% Error	ANN Distance (in kms)	% Error
1.	55	52.82	0.917	52.57	1.056	52.14	1.243	55.78	0.340
2.	95	95.03	0.013	94.18	0.356	94.69	0.310	93.74	0.548
3.	135	134.99	0.004	134.98	0.008	134.98	0.020	134.96	0.017
4.	175	175.01	0.004	175.00	.000	174.98	0.009	174.98	0.009
5.	215	214.93	0.030	215.09	0.039	214.98	0.009	215.00	0.000

Table 3.16: Performance of ANN using Bus-2 Data as Inputs for Solid Faults

S.No.	Actual Distance (in kms)	Phase-C to Ground Fault (CG)		Phase-A to Phase-C Fault (AC)		Phases-AC to Ground Fault (ACG)		Three-Phase Fault (ABCG)	
		ANN Distance (in kms)	% Error	ANN Distance (in kms)	% Error	ANN Distance (in kms)	% Error	ANN Distance (in kms)	% Error
1.	55	56.90	0.826	55.64	0.278	61.87	2.987	58.58	1.557
2.	95	93.50	0.652	95.25	0.108	94.37	0.274	94.39	0.265
3.	135	134.95	0.021	135.05	0.021	135.02	0.009	134.94	0.261
4.	175	175.03	0.013	175.01	0.004	175.00	0.000	174.92	0.348
5.	215	214.89	0.478	215.21	0.091	214.98	0.008	214.79	0.091

Table 3.17: Performance of ANN using Bus-2 Data as Inputs for High Impedance Faults (Z_f=15 Ω)

S.No.	Actual Distance (in kms)	Phase-C to Ground Fault (CG)		Phase-A to Phase-C Fault (AC)		Phases-AC to Ground Fault (ACG)		Three-Phase Fault (ABCG)	
		ANN Distance (in kms)	% Error	ANN Distance (in kms)	% Error	ANN Distance (in kms)	% Error	ANN Distance (in kms)	% Error
1.	55	56.15	0.217	54.75	0.108	59.49	1.952	54.36	0.278
2.	95	94.08	0.400	94.76	0.104	94.72	0.122	94.62	0.165
3.	135	134.90	0.043	134.98	0.009	135.02	0.009	134.99	0.004
4.	175	174.98	0.009	175.01	0.004	175.03	0.013	174.94	0.026
5.	215	215.05	0.021	214.89	0.478	215.09	0.040	214.87	0.057

Table 3.18: Performance of ANN using Local and Remote Bus Data as Inputs for Solid Faults

S.No.	Actual Distance (in kms)	Phase-A to Ground Fault (AG)		Phase-A to Phase-B Fault (AB)		Phases-A and B to Ground Fault (ABG)		Three-Phase Fault (ABCG)	
		ANN Distance (in kms)	% Error	ANN Distance (in kms)	% Error	ANN Distance (in kms)	% Error	ANN Distance (in kms)	% Error
1.	55	54.72	0.122	55.00	0.000	54.93	0.030	55.42	0.183
2.	95	95.01	0.004	94.99	0.004	95.26	0.113	95.61	0.265
3.	135	134.99	0.004	135.10	0.043	135.09	0.391	134.75	0.109
4.	175	175.25	0.109	175.72	0.313	176.09	0.474	176.13	0.491
5.	215	214.47	0.230	218.49	1.517	217.78	1.208	215.14	0.061

Table 3.19: Performance of ANN using Local and Remote Bus Data as Inputs for High Impedance Faults (Z_f=15 Ω)

S.No.	Actual Distance (in kms)	Phase-A to Ground Fault (AG)		Phase-A to Phase-B Fault (AB)		Phases-A and B to Ground Fault (ABG)		Three-Phase Fault (ABCG)	
		ANN Distance (in kms)	% Error	ANN Distance (in kms)	% Error	ANN Distance (in kms)	% Error	ANN Distance (in kms)	% Error
1.	55	54.67	0.143	54.70	0.130	54.83	0.074	55.03	0.013
2.	95	94.97	0.130	95.06	0.026	95.19	0.083	95.26	0.113
3.	135	135.00	0.000	135.06	0.026	135.07	0.030	134.93	0.030
4.	175	175.03	0.013	175.53	0.230	176.03	0.448	175.36	0.157
5.	215	215.41	0.178	215.93	0.404	217.47	1.074	217.21	0.961

.Table 3.20: Errors for different ANNs

Input Data	Average % Error	Maximum % Error
Bus-1	0.309	2.730
Bus-2	0.328	2.987
Bus-1 and Bus-2	0.240	1.517

3.7 CONCLUSION

A wavelet-alienation based approach can be successfully used for detection, classification and location of faults on two-terminal transmission lines. Fault detection and classification have been achieved within a quarter cycle using alienation of wavelet based approximate coefficients of three-phase currents obtained from both the terminals. The ANNs, fed from approximate coefficients, obtained over a quarter cycle of post fault voltage and current signals, can be utilized to locate the fault precisely with an average error of 0.24%. The proposed protection scheme has been tested successfully for all the types of fault with variation in location, inception angle and fault impedance.